
Green Hierarchical Vision Transformer for Masked Image Modeling

Lang Huang¹, Shan You^{2*}, Mingkai Zheng³, Fei Wang², Chen Qian², Toshihiko Yamasaki¹

¹The University of Tokyo; ²SenseTime Research; ³The University of Sydney

{langhuang,yamasaki}@cvm.t.u-tokyo.ac.jp

{youshan,wangfei,qianchen}@sensetime.com

Abstract

We present an efficient approach for Masked Image Modeling (MIM) with hierarchical Vision Transformers (ViTs), allowing the hierarchical ViTs to discard masked patches and operate only on the visible ones. Our approach consists of three key designs. First, for window attention, we propose a Group Window Attention scheme following the Divide-and-Conquer strategy. To mitigate the quadratic complexity of the self-attention w.r.t. the number of patches, group attention encourages a uniform partition that visible patches within each local window of arbitrary size can be grouped with equal size, where masked self-attention is then performed within each group. Second, we further improve the grouping strategy via the Dynamic Programming algorithm to minimize the overall computation cost of the attention on the grouped patches. Third, as for the convolution layers, we convert them to the Sparse Convolution [25, 13] that works seamlessly with the sparse data, *i.e.*, the visible patches in MIM. As a result, MIM can now work on most, if not all, hierarchical ViTs in a **green** and efficient way. For example, we can train the hierarchical ViTs, *e.g.*, Swin Transformer [49] and Twins Transformer [14], about $2.7\times$ faster and reduce the GPU memory usage by 70%, while still enjoying competitive performance on ImageNet classification and the superiority on downstream COCO object detection benchmarks.[†]

1 Introduction

Driven by the great success of Masked Language Modeling (MLM) [56, 57, 15, 6] in natural language processing (NLP) and the advancement of Vision Transformers (ViTs) [17, 49, 66, 77], Masked Image Modeling (MIM) emerged as a promising self-supervised pre-training paradigm for computer vision (CV). MIM learns representations from unlabelled data by masked prediction, *e.g.*, predicting the discrete tokens [3], the latent features [81, 68, 2], or the raw pixels [28, 73] of the randomly masked input image patches. Among them, the representative work Masked Autoencoder (MAE) [28] exhibited competitive performance as well as impressive efficiency. In essence, MAE proposed an asymmetric encoder-decoder architecture for MIM, where the encoder (*e.g.*, a standard ViT model [17]) operates only on visible patches, and the light-weight decoder recovers all patches for mask prediction.

On the one hand, the asymmetric encoder-decoder architecture significantly reduces the computation burden of pre-training. On the other hand, MAE only supports the isotropic ViT [17] architecture as the encoder, while most of the modern vision models adopt hierarchical structure [43, 31, 49], in part due to the need of handling the scale-variations of visual elements. In fact, the hierarchical structure and local inductive bias are crucial in various CV tasks that require representations of different levels

*Corresponding author. [†]Code and pre-trained models: <https://github.com/LayneH/GreenMIM>.

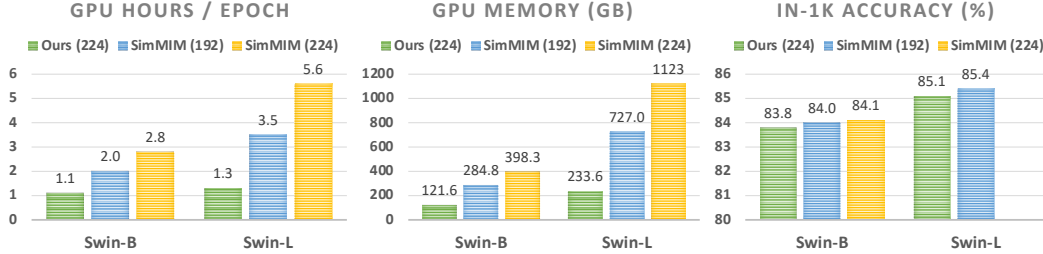


Figure 1: **Comparison with SimMIM in terms of efficiency.** All methods use a Swin-B/Swin-L backbone and batch size of 2,048. The experiments of our method are conducted on a single machine with eight V100 GPUs, CUDA 10, and PyTorch 1.8, while those of SimMIM require 2 or 4 machines.

or scales to make predictions, including image classification [31], and object detection [22]. Yet it is still not straightforward how the hierarchical vision transformers, *e.g.* Swin Transformer [49], can be integrated into the MAE framework. Moreover, though the work SimMIM [73] has explored Swin Transformer for MIM, it operates on both visible and masked patches and suffers from heavy computation costs compared with MAE. As a concrete example, we find that even the base size model of SimMIM cannot be trained on a single machine with eight 32GB GPUs, let alone the larger ones. The computation burden makes it difficult for a wider range of researchers to dive into this field of research, not even to mention the amount of carbon emission during the model development process.

To this end, we strive to devise a new and green approach for MIM with hierarchical models, in the spirit of *Green AI* [61, 74]. Our work focuses on extending the asymmetric encoder-decoder architecture of MAE to hierarchical vision transformers, particularly the representative model Swin Transformer [49], for the sake of efficient pre-training on visible patches only. We identify that the major obstacle is the inductive bias of hierarchical ViTs, *i.e.*, the locality induced by i) window attention [36, 49, 77] with non-overlapped window partition, and ii) convolution/pooling [66, 19, 14, 27] with overlapped window partition. These operators are incompatible with random masking as it creates various-sized local windows that are infeasible for computing in parallel.

This paper provides the first attempt to address this drawback. We present a *Green* Hierarchical Vision Transformer for Masked Image Modeling that advocates a more practical method with drastically improved efficiency. Our methodology is conceptually simple and consists of three key designs.

1. Guided by the Divide-and-Conquer principle, we present a Group Window Attention scheme first partitioning the local windows with uneven numbers of visible patches into several equal-sized groups and then applying the masked attention within each group.
2. We formulate the aforementioned group partition as a constrained optimization problem, where the objective is to find a group partition that minimizes the computation cost of the attention on the grouped tokens. Inspired by the concept of Dynamic Programming [5] and the greedy principle, we propose an Optimal Grouping algorithm that adaptively selects the optimal group size and partitions the local windows into a minimum number of groups.
3. We convert the convolution layers in the hierarchical ViTs to the Sparse Convolution [25, 13, 1], which was originally designed for handling sparse point cloud data and works seamlessly with the masked inputs in MIM.

Our methodology is generic and does not make *any* modification to the architecture of the backbone models, such that we can make apple-to-apple comparisons with the baseline operating on both visible and masked patches. In our experimental evaluations, we observed that our method requires substantially less training time and consumes much less GPU memory while performing on par with the baseline on both ImageNet1K [60] classification and MS-COCO [47] object detection. Concretely, using Twins-L [14]/Swin-B [49]/Swin-L [49], our method achieves up to $2.7\times$ speedup and consumes as few as 30% of GPU memory compared with the baseline SimMIM at the pre-training stage, while achieving 83.9%/83.8%/85.1% top-1 fine-tuning accuracy on the ImageNet-1K that is on par with those of SimMIM.

2 Related Works

Self-Supervised Learning. Representation learning is a long-standing and fundamental question in CV. For a long time, representation learning had been dominated by supervised learning. Until recent three years, self-supervised learning (SSL) exhibited impressive performance and attained significant attention. Generally, SSL solves a proxy task without the actual interest to learn good representations. According to the proxy tasks, SSL methods can be categorized into generative approaches and discriminative approaches. Generative approaches predict the original data based on the partially observed inputs [65, 55, 44], predict the transformation applied to the input [52, 21], or model pixels in the input space [42, 23, 39, 33]. Masked Image Modeling also falls into this category. Discriminative approaches received more interest during the past few years, especially the contrastive learning methods. Contrastive learning creates multiple views of images with a set of random data distortions and encourages the representations to be invariant to the distortions. A large number of contrastive learning approaches [70, 53, 29, 10, 79, 80] drive the training by maximizing the similarities between positive samples (*i.e.*, views from the same image) while minimizing those between the negative samples, and some works simply get rid of the negative pairs [26, 7, 11, 37, 78, 8]. Beyond contrastive learning on global features, several methods proposed to maintain the spatial information of representations and use region/mask/pixel-level contrastive learning [67, 72, 71, 32, 35].

Masked Language/Image Modeling. Self-supervised pre-training has revolutionized the NLP. Among them, the Masked Language Modeling (MLM) proposed in BERT [15] and its variants [6] are the most dominant methods, which learn representations by predicting the tokens that are randomly masked in the input sentence. Masked Image Modeling has a similar idea of predicting corrupted images, and some of these methods [65, 55] were proposed Even preceded to BERT. These methods were, however, unable to perform on par with other pre-training paradigms at that time. Until recently, aided by the significant advancement of Vision Transformers [17], several MIM methods presented promising results [17, 3, 28, 73, 68] and became the state-of-the-art of self-supervised learning in CV. These methods can be roughly differentiated in terms of the prediction target, *e.g.*, color bins [17], discrete tokens [3, 16] from pre-trained VAEs [63, 58], raw pixels [28, 73], and handcrafted features [68]. Among these approaches, MAE [28] exhibited competitive performance as well as impressive efficiency as it discards the masked tokens and operates only on the visible ones.

Isotropic and Hierarchical Vision Transformers. The seminal work Vision Transformer (ViT) [17] revolutionized the conventional view of images. ViT, and its variant [62], treat an image as a sequence of patches and adopt a pure Transformer [64] backbone to model the patches for image classification, achieving an impressive performance even compared with the Convolutional Neural Networks. Nevertheless, while the results of ViT are promising in classification, its performance on dense prediction tasks is less favorable, which is largely due to its low-resolution feature maps inherited from its isotropic structure and the quadratic complexity of self-attention [64]. To this end, a strand of works proposed hierarchical structure [66, 49, 19, 77], efficient attention [36, 49, 14, 38], and locality bias [18, 69, 27, 76] for ViTs, unleashing the potential of ViTs as general-purpose vision backbones. Our work performs studies upon the representative hierarchical ViTs, Swin Transformer [49] and Twins Transformer [14] but generalizes to any other ViTs with window local attention or convolution/pooling.

Green AI. Witnessing the exponential growth of computations of big AI models [15, 6, 48], the concept of **Green AI** attains mounting attention in recent years [61, 74]. Rather than being merely obsessed with accuracy, **Green AI** advocates making efficiency an important measure of AI models, championing the greener approaches that are more inclusive to the research community. This work follows the path of **Green AI** and presents a greener approach for MIM with hierarchical ViTs.

3 Approach

3.1 Preliminary

Notations. Let $\mathbf{X} \in \mathbb{R}^{C \times H \times W}$ denote the input feature where C , H , and W are the numbers of channels, height, and width of \mathbf{X} ; $\mathbf{M} \in \{0, 1\}^{H \times W}$ denotes the (spatial) mask generated randomly during training where 0 indicates a patch is invisible for the encoder, and vice versa.

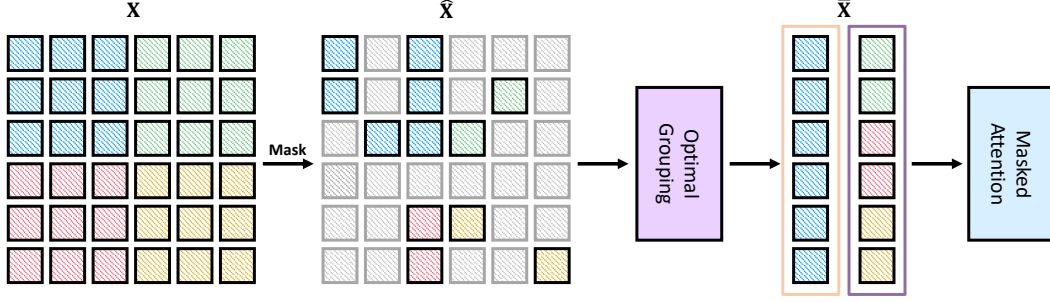


Figure 2: **Illustration of the Group Window Attention scheme.** In Masked Image Modeling (MIM), the input \mathbf{X} , where different colors indicate the tokens belong to different local windows, is randomly masked, producing $\hat{\mathbf{X}}$ of which most tokens are invisible. Our Group Window Attention first performs an optimal grouping to group the visible tokens of the local windows into several equal-sized groups, forming $\bar{\mathbf{X}}$. Finally, we perform the Masked Attention within each group to ensure no inter-window information leakage.

Masked Image Modeling. MIM learns representations by predicting the masked portion of a input \mathbf{X} from its partial observation $\hat{\mathbf{X}} \leftarrow \text{Mask}(\mathbf{X}, \mathbf{M})$. Existing MIM methods fall into two categories regarding the $\text{Mask}(\cdot, \cdot)$ operation. Most methods [3, 73, 68] use the Hadamard product for masking and retain the masked patches, *i.e.*, $\hat{\mathbf{X}} \leftarrow \text{Mask}(\mathbf{X}, \mathbf{M}) = \mathbf{X} \odot \mathbf{M}$ with \mathbf{M} broadcasted for C times along the channel dimension. In sharp contrast to these methods, Masked Autoencoders (MAE) [28] proposes throwing the masked patches at the masking stage, *i.e.*,

$$\hat{\mathbf{X}} \leftarrow \text{Mask}(\mathbf{X}, \mathbf{M}) = \{\mathbf{X}_{i,j} : \mathbf{M}_{i,j} = 1\}. \quad (1)$$

MAE designs an asymmetric and isotropic encoder-decoder architecture to take advantage of partial inputs: the encoder operates only on the visible patches $\hat{\mathbf{X}}$ without mask tokens; the decoder reconstructs the original images from representations of visible patches and masked tokens. This design allows MAE to achieve competitive performance as well as impressive efficiency, *e.g.*, $3\times$ training speedup compared with the ones operating on all patches. Nevertheless, the MAE works only with the isotropic ViTs and it is unclear *how to translate the efficiency of MAE to hierarchical ViTs*, which exhibited nearly unanimous superiority over the isotropic ones on most vision tasks [66, 49, 19, 14, 77]. In this paper, we attempt to answer this question and propose a much **greener** approach for MIM with Hierarchical ViTs.

3.2 Green Hierarchical Vision Transformer for Masked Image Modeling

Adapting existing hierarchical ViTs for MIM. A typical hierarchical ViT mainly consists of Feed-Forward Networks (FFNs) and efficient attentions, which fail to operate only on the visible patches. We identify that the major obstacle is the inductive bias of hierarchical ViTs, *i.e.*, the locality induced by i) window attention [36, 49, 77] with non-overlapped window partition, and ii) convolution/pooling [66, 19, 14, 27] in FFNs or attentions with overlapped window partition. These operators are incompatible with random masking as it creates various-sized local windows that are infeasible for computing in parallel. To this end, we present two key insights to make most, if not all, hierarchical ViTs be able to operate only on visible patches in a **green** manner.

Group Window Attention. Regarding the non-overlapped window partition, we propose a Group Window Attention scheme that significantly improves the computation efficiency of window attention on masked features. Given the masked feature $\hat{\mathbf{X}} = \text{Mask}(\mathbf{X}, \mathbf{M})$ following Equation (1), we collect a set of uneven local windows $\hat{\mathbf{X}} \rightarrow \{\hat{\mathbf{X}}_i\}_{i=0}^{n_w}$ of which each element contains the visible tokens only, with sizes $\{w_i\}_{i=0}^{n_w}$ accordingly. As shown in Figure 2, our Group Window Attention first uses an Optimal Grouping algorithm to partition the uneven windows into several equal-sized groups and then performs Masked Attention within each group to avoid information leakage. In the next two subsections, we will elaborate on these two components, respectively.

Incorporating with Sparse Convolution. Our intuition is the features of mask inputs can be viewed as sparse tensors where only features of (a small number of) visible patches are retained while

Algorithm 1 Optimal Grouping

Require: The number of visible patches within each local window $\{w_i\}_{i=0}^{n_w}$,

```
1: Minimum computational cost  $c^* \leftarrow +\infty$ 
2: for  $g_s = \max_i \{w_i\}_{i=1}^{n_w}$  to  $\sum_{i=1}^{n_w} w_i$  do
3:   Remaining windows  $\Phi \leftarrow \{w_i\}_{i=1}^{n_w}$ ; partition  $\Pi \leftarrow \emptyset$ ; the number of group  $n_g \leftarrow 0$ 
4:   repeat
5:      $\pi_{n_g} \leftarrow \text{Knapsack}(g_s, \Phi)$ , as in Equation (7)
6:      $\Pi \leftarrow \Pi \cup \pi_{n_g}$ ;  $\Phi \leftarrow \Phi \setminus \pi_{n_g}$ 
7:      $n_g \leftarrow n_g + 1$ 
8:   until  $\Phi = \emptyset$ 
9:    $c \leftarrow \mathcal{C}(g_s, \Pi)$ , as in Equation (8)
10:  if  $c < c^*$  then
11:     $c^* \leftarrow c$ ;  $\Pi^* \leftarrow \Pi$ 
12:  end if
13: end for
14: return Optimal group partition  $\Pi^*$ 
```

the others are omitted. From this perspective, we propose to directly replace all the convolution/pooling operations in hierarchical ViTs with the highly optimized Sparse Convolution [24, 25, 13, 1], originally designed for the sparse 3D point cloud data.

3.3 Optimal Grouping with Dynamic Programming

General formulation. The first step of the optimal grouping is to find an indexes partition Π with respect to the group size g_s :

$$\Pi = \{\pi_j\}_{j=1}^{n_g}, \quad (2)$$

$$s.t. \cup_j \pi_j = \{1, \dots, \sum_i w_i\}, \sum_j |\pi_j| = \sum_i w_i, \text{ and } \forall_j \sum_{k \in \pi_j} w_k \leq g_s. \quad (3)$$

where n_g is the number of resulting groups. The conditions in Equation (3) constrain the partition to contain all local windows with no duplicate and enforce the actual size of each group to be smaller than g_s . Based on the partition Π , we obtain a set of grouped tokens $\{\bar{\mathbf{X}}_j\}_{j=1}^{n_g}$ that

$$\bar{\mathbf{X}}_j = \text{Concat}(\{\hat{\mathbf{X}}_k : \forall k \in \pi_j\}), \quad \bar{\mathbf{X}}_j \in \mathbb{R}^{C \times g_s},^2 \quad (4)$$

upon which the Masked Attention is performed. Finally, we apply the inverse operation of the partition Π to recover the positions of output tokens.

With the formulation above, there remain two questions unresolved: 1) how to choose the optimal group size g_s^* , and 2) how to obtain the optimal partition Π^* given g_s^* . To this end, we formulate our objectives as the below min-min optimization problem,

$$g_s^* = \underset{g_s}{\text{argmin}} \mathcal{C}(g_s, \text{Partition}(g_s, \{w_i\}_i)), \quad (5)$$

$$\text{Partition}(g_s, \{w_i\}_{n_w}) = \underset{\Pi}{\text{argmin}} |\Pi|, \text{ s.t. Equation (3)}, \quad (6)$$

where $\mathcal{C}(\cdot)$ is a cost function measuring the computation cost of the attention with the grouped tokens. Intuitively, Equation (5) aims to find the optimal group size g_s^* that the computation cost of the optimal partition w.r.t. g_s^* is the minimum. Equation (6) searches for the optimal partition, with the constraints of Equation (3). Having the optimal group size, we can directly obtain the optimal partition $\Pi^* = \text{Partition}(g_s^*, \{w_i\}_{n_w})$. Next, we will present in detail how we solve the above optimization problem.

Group partition with Dynamic Programming. We find that the optimization problem in Equations (6) and (3) is a special case of the multiple subset sum problem with identical capacities (MSSP-I), a variant of the well-known 0-1 multiple knapsack problem with identical capacities (MKP-I) [40, Chapter 10]. In our case, the group size is analogous to the capacity of knapsacks, the

²Here we assume the number of tokens $\sum_i w_i$ is divisible by g_s for simplicity. In practice, we pad the group π_j when $|\pi_j|$ is smaller than g_s .

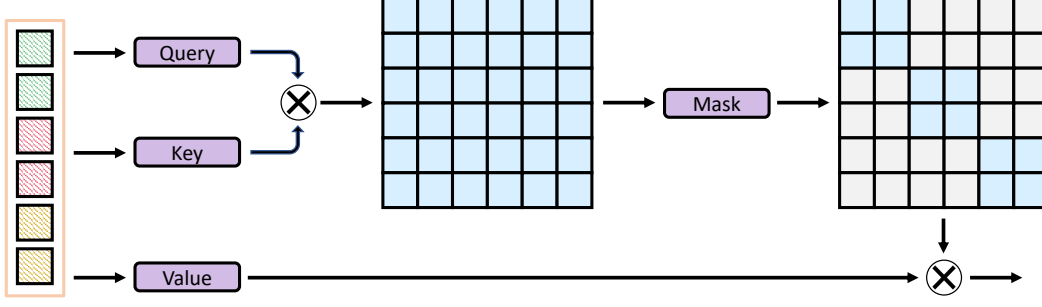


Figure 3: **Illustration of the Masked Attention scheme.** Given a group of tokens, we first compute their pairwise attention weights and then set the attention weights between tokens from different local windows to $-\infty$ (indicated by the gray cells). The final attention output is then computed with the masked attention map.

numbers of visible tokens $\{w_i\}_{n_w}$ are analogous to the values of goods, the weights of goods are the same as their values, and the number of knapsacks is unbounded. Although MSSP-I is strictly NP-complete, there exist multiple polynomial time approximation schemes for it, *e.g.*, using the dynamic programming (DP) algorithms [5]. Specifically, we make use of the DP algorithm for the single knapsack problem (or the subset sum problem):

$$\pi \leftarrow \text{Knapsack}(g_s, \Phi), \quad (7)$$

which selects a subset π that $\sum_{u \in \pi} |u| \leq g_s$ out of the full set Φ (the pseudo-code of this algorithm is given in Appendix). We alternatively apply this algorithm to the remaining full set Φ and exclude the selected subset π from Φ , until Φ is empty. In practice, we found that our algorithm is very fast and the time cost is negligible because the number of local windows is often small, *e.g.*, less than 100 in our pre-training stage.

Cost function. Because we mainly care about the efficiency, we use the FLOPs to measure the computation complexity of the multi-head attention on grouped tokens, *i.e.*,

$$\mathcal{C}(g_s, \Pi) = |\Pi| \times (4g_s C^2 + 2g_s^2 C) = n_g \times (4g_s C^2 + 2g_s^2 C), \quad (8)$$

where C is the number of channels. Although the complexity is quadratic w.r.t. the group size g_s , using smaller g_s might produce more groups (and more padding) and suffers from suboptimal efficiency. Therefore the optimal group size is determined adaptively during training.

Putting everything together. We sweep over the possible values of group size, from $\max_i w_i$ to $\sum_i w_i$, to find the optimal group size. For each selected group size, we firstly use the DP algorithm in Equation (7) to partition the windows and then calculate the computation cost of the attention this partition. The one with minimum cost is chosen as the optimal group size. The pseudo-code of the optimal grouping is summarized in Algorithm 1.

3.4 Masked Attention

Because non-adjacent local windows are partitioned into the same groups, masking the attention weights is needed to avoid the information exchange between these local windows. As illustrated in Figure 3, having computed the attention map, we retain only the intra-window attention weights (*i.e.*, the block-diagonal elements) and discard the inter-window ones. A similar masking scheme is also applied to the retrieving of relative position bias [49], where we store the original absolute position of each token and compute the relative positions on-the-fly to retrieve the corresponding biases.

3.5 Batch-wise Random Masking

We observed that the per-sample random masking strategy would deteriorate the efficiency of our method: 1) it might produce different numbers of groups of local windows for each sample, which is intractable for the parallel computation of the Masked Attention; 2) when the mask patch size is smaller than the largest patch size of the hierarchical models, some patches might contain both visible

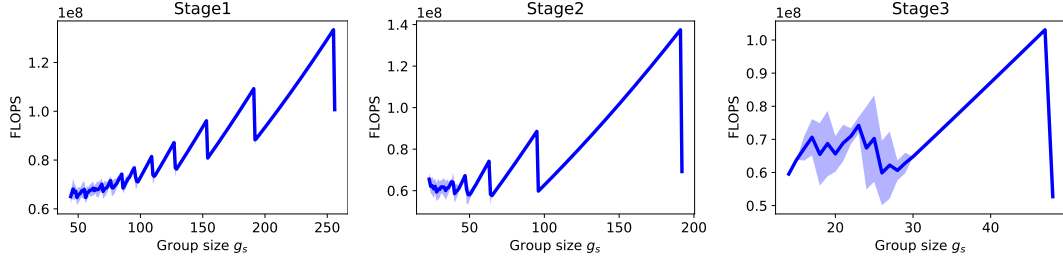


Figure 4: **The optimal group size g_s at each stage.** The figure of the fourth stage is omitted here because there is only one local window in this stage, so the grouping is not necessary. The simulation is repeated 100 times, of which the mean and standard deviation (the shaded regions) are reported.

and masked inputs. In this case, we can not discard such patches during training and fail to fully take advantage of the sparsification. Therefore, we propose to set the mask patch size to the same value as the largest patch size of the encoder (e.g., 32 for most hierarchical models, which is also the default choice of [73]) and use the same random mask for all samples in the same GPU device (a.k.a., a micro-batch).

4 Experiments

4.1 Implementation Details and Experimental Setups

We conduct experiments on the ImageNet-1K [60] (BSD 3-Clause License) image classification dataset and MS-COCO [47] (CC BY 4.0 License) object detection/instance segmentation dataset. The Swin-Base, Swin-Large [49] and Twins-Large [14] models, which consist of four stages with features of stride 4/8/16/32, are used as the encoder throughout this paper, allowing for direct comparisons with the baseline SimMIM [73] with Swin Transformer. The models are first pre-trained on the ImageNet-1K dataset without label and then fine-tuned on downstream tasks. All the experiments of our method are performed on a single machine with eight 32G Tesla V100 GPUs, CUDA 10.1, PyTorch [54] 1.8, and automatic mixed-precision training [51]. For the experiments involving convolution, we replace all the standard convolutions with the sparse convolution implemented in [1] as discussed in Sec. 3.2.

Pre-training setup. We patchify images of size 224×224 with a patch size of 4×4 and randomly mask the patches with a ratio r ($r = 0.75$ by default) following the scheme in Section 3.5. The input images are first transformed by a set of simple data augmentations, including random cropping and horizontal flip, and standardization. Following the prior work MAE [28], we adopt a lightweight decoder that consists of n_d (by default $n_d = 1$) standard transformer blocks with an embedding dimension of 512. The decoder takes the representations of visible patches and the mask token as input and is appended after the final stage of the encoder to learn representations for the masked patches. It is followed by a linear layer to predict the normalized pixel values of the masked patches. The models are trained for 100/200/400/800 epochs with a total batch size of 2,048. We use the AdamW optimizer [41] with the cosine annealing schedule [50]. We set the base learning rate to $1.5e^{-4}$, the weight decay to 0.05, the hyper-parameters of Adam $\beta_1 = 0.9$, $\beta_2 = 0.999$, the number of warmup epochs to 40 with an initial base learning rate $1.5e^{-7}$. The effective learning rate is scaled linearly by $\text{batch_size}/256$.

Fine-tuning on the ImageNet-1K dataset. For fine-tuning, we drop the decoder and directly append a 1,000-way fully-connected layer to the average-pooled output of the encoder as the classifier. The models are also optimized by the AdamW optimizer [41] with 100 training epochs in total, 20 warmup epochs, a base/warmup learning rate of $1.25e^{-4}/2.5e^{-7}$, the cosine annealing schedule [50], a weight decay of 0.05. A layerwise learning rate decay [3] of 0.9/0.8/0.9, and a stochastic depth [34] ratio of 0.2/0.3/0.2 are used for Swin-B/Swin-L/Twins-L respectively. The data augmentations are the same as [3, 73].

Fine-tuning on the MS-COCO dataset. We adopt the Mask R-CNN [30] architecture with the FPN [46] as the detector. All models are fine-tuned on the MS-COCO [47] 2017 train split ($\sim 118k$ images) and finally evaluated on the val split ($\sim 5k$ images). We use a batch size of 16, AdamW

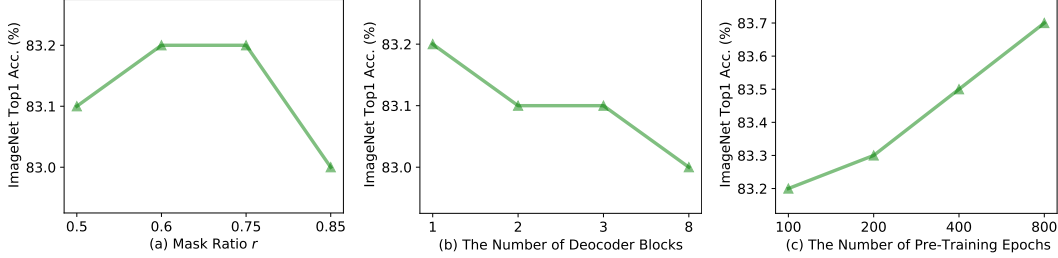


Figure 5: **Ablation studies of** (a) the choice of the mask ratio r , (b) the number of transformer blocks n_d in the decoder, and (c) the number of pre-training epochs.

optimizer [41] with a learning rate of $1e^{-4}$, a weight decay of 0.05. The $1\times/3\times$ schedule in the mmdetection [9] is adopted, which uses 12/36 training epochs in total and decays the learning rate at the $\frac{3}{4}$ and $\frac{11}{12}$ of the total epochs by a factor of 10. The standard COCO metrics, including AP, AP₅₀, and AP₇₅ for both object detection and instance segmentation are used for evaluation.

4.2 Ablations studies

Efficiency comparison with SimMIM. We compare the efficiency of our method to the baseline SimMIM in Figure 1. The evaluations are performed on a single machine with eight 32GB V100 GPUs for our method and on 2 or 4 machines for the SimMIM because it fails to fit into a single machine with the default batch size of the original paper [73] (*i.e.*, 2,048). As we can see from the figures, the training of SimMIM with images of size 224^2 is very slow and memory-hungry. Although training with smaller images considerably reduces the training time and memory consumption, it still far lags behind our method with images of size 224^2 . Concretely, with the same amount of training epochs, our method performs on par with baseline with $\sim 2\times$ speedup and $\sim 60\%$ of memory reduction using Swin-B. We also observe that the efficiency improvements become larger with the larger Swin-L, *e.g.*, $2.7\times$ speedup compared with SimMIM₁₉₂, highlighting the efficiency of our method with larger models. In addition, the efficiency comparison using Twins Transformer is presented in Appendix A.1 for completeness, which exhibits similar superiority of our approach.

The optimal group size g_s on each stage. Because hierarchical models have multiple stages with different scales of features, the optimal group size of each stage might also be different. Regarding this, we design a simulation experiment to analyze the optimal g_s at different stages. In the simulation, we randomly generate 100 masks following Section 3.5, compute the costs w.r.t. different choices of g_s , and report the mean/standard deviation of the costs in Figure 4. Note that the analysis of the 4th stage is omitted here because it only has one local window. In general, we observed that the cost increases quadratically w.r.t. the group size, except for some cases where the group size is exactly equal to the sum of a subset of local windows. Another intriguing observation is that the cost at each stage seems to be the minimum around the point that $g_s = 49$, which is equal to the window size of the window attention. This observation indicates that we may not need to sweep over all possible group sizes but simply set $g_s = p \times p$ in practice. Moreover, we analyze the influence of the optimal grouping and the cost of each part of it in Appendix A.2, showing that optimal grouping is indeed crucial for the efficiency of our method.

The influence of the mask ratio, the number of decoder blocks, and the pre-training epochs. From Figure 5(a), we can see that the performance of our method is quite stable with the mask ratio r varying from 0.5 to 0.85, which conforms with the observation of [28]. In Figure 5(b), we also study the influence of the depth of the decoder. Intriguingly, the results suggest that fewer decoder blocks produce better results. This study favors the simple prediction head design of SimMIM [73] with hierarchical models and is in contrast to the observation of MAE [28] with isotropic ones. For simplicity and efficiency, we fix $r = 0.75$ and the number of decoder blocks to 1 throughout the paper. Furthermore, we study the impact of pre-training budgets on our method. As shown in Figure 5(c), the fine-tuning accuracy increases steadily w.r.t. the number of training epochs and does not seem to stagnate, suggesting its potential for a further performance boost.

Pre-training with larger window size. The work of [48] puts forth that using a larger window size is beneficial for fine-tuning. In practice, however, it might be less practical because of the

Table 2: Top1 accuracy on the ImageNet-1K validation set with the Swin-B or ViT-B models. All methods are trained with images of size 224×224 in both the pre-training and fine-tuning except for SimMIM₁₉₂ using 192×192 in the pre-training.

Method	Model	#Params	PT Ep.	Ep. Hours	Total Hours	FT Ep.	Acc. (%)
<i>Training from scratch</i>							
Scratch, DeiT [62]	ViT-B	86M	0	-	-	300	81.8
Scratch, MAE [28]	ViT-B	86M	0	-	-	300	82.3
Scratch, Swin [49]	Swin-B	88M	0	-	-	300	83.5
Scratch, Twins [14]	Twins-L	99M	0	-	-	300	83.7
<i>Supervised Pre-training</i>							
Supervised, SimMIM [73]	Swin-B	88M	300	-	-	100	83.3
Supervised, SimMIM [73]	Swin-L	197M	300	-	-	100	83.5
<i>Pre-training with Contrastive Learning</i>							
MoCov3 [12]	ViT-B	86M	800	-	-	100	83.2
DINO [8]	ViT-B	86M	800	-	-	100	82.8
<i>Pre-training with Masked Image Modeling</i>							
BEiT [3]	ViT-B	86M	800	-	-	100	83.2
MaskFeat [68]	ViT-B	86M	800	-	-	100	84.0
MAE [28]	ViT-B	86M	1600	1.3	2069	100	83.6
SimMIM ₂₂₄ [73]	ViT-B	86M	800	4.1	3307	100	83.8
SimMIM ₁₉₂ [73]	Swin-B	88M	800	2.0	1609	100	84.0
SimMIM ₁₉₂ [73]	Swin-L	197M	800	3.5	2821	100	85.4
Ours	Swin-B	88M	800	1.1	887	100	83.8
Ours	Twins-L	99M	800	0.8	676	100	83.9
Ours	Swin-L	197M	800	1.3	1067	100	85.1

quadratic complexity of self-attention w.r.t. the window size. Fortunately, operating only on the visible patches permits the training with a larger window size with little extra cost. As displayed in Table 1, pre-training with doubled window size only marginally increases the training time/GPU memory by less than 10%/20% yet brings a moderate performance improvement despite $p = 7$ in the fine-tuning stage.

Table 1: A larger window size $p \times p$.

$p \times p$	Time	Mem.	Acc.
7×7	1.1h	121.6G	83.2%
14×14	1.2h	148.9G	83.4%

4.3 ImageNet-1K Classification

We fine-tune the pre-trained models on the ImageNet-1K dataset and report the results on the validation set in Table 2. Here, we make direct comparisons with the models 1) trained from scratch with a longer training schedule, 2) trained with contrastive learning, and 3) trained with other MIM approaches. Our approach achieves 83.8%/83.9%/85.1% top-1 fine-tuning accuracy with the Swin-B/Twins-L/Swin-L backbone, which is clearly superior to the supervised learning/contrastive learning methods and on par with other MIM methods using backbones with similar capacities. The results demonstrate the effectiveness of our method, in addition to the substantial efficiency improvements over both MAE and SimMIM.

4.4 MS-COCO Object Detection and Instance Segmentation

Finally, we evaluate the transfer learning performance of our pre-trained models to the MS-COCO object detection and instance segmentation dataset. Here, we directly use the code base of the supervised Swin Transformer without any modification to the fine-tuning strategy. For direct comparisons, we reran the experiments for the supervised Swin-B and SimMIM using their public checkpoints. The experiment results are summarized in Table 3. Compared with the supervised pre-trained Swin-B, our approach performs prominently better in terms of all metrics, *e.g.*, 1.5% absolute improvement in AP^b. In addition, we also observed that our approach still performs comparably to the SimMIM on dense prediction tasks. More significantly, our approach outperforms most of the baselines from [45] using $3\times$ or $10\times$ more fine-tuning epochs and advanced data augmentations [20]. These experiments,

Table 3: **MS-COCO object detection and instance segmentation.** All methods are based on the Mask R-CNN [30] architecture with the FPN [46] neck. The methods in gray are cited from [45]. Most of them use much longer training schedules and advanced data augmentations.

Method	Backbone	PT Ep.	PT Hours	FT Ep.	AP ^b	AP ^b ₅₀	AP ^b ₇₅	AP ^m	AP ^m ₅₀	AP ^m ₇₅
<i>Training from scratch</i>										
Benchmarking [45]	ViT-B	0	0	400	48.9	-	-	43.6	-	-
<i>Supervised Pretraining</i>										
Benchmarking [45]	ViT-B	300	992	100	47.9	-	-	42.9	-	-
PVT [66]	PVT-L	300	-	36	44.5	66.0	48.3	40.7	63.4	43.7
Swin [49]	Swin-B	300	840	36	48.5	69.8	53.2	43.2	66.9	46.7
<i>Self-Supervised Pre-training</i>										
MoCov3 [12]	ViT-B	800	-	100	47.9	-	-	42.7	-	-
BEiT [3]	ViT-B	800	-	100	49.8	-	-	44.4	-	-
MAE [28]	ViT-B	1600	2069	25	48.1	-	-	-	-	-
MAE [28]	ViT-B	1600	2069	100	50.3	-	-	44.9	-	-
SimMIM [73]	Swin-B	800	1609	36	50.4	70.9	55.5	44.4	68.2	47.9
Ours	Swin-B	800	887	36	50.0	70.7	55.4	44.1	67.9	47.5

combined with the results in Table 2, verify that our approach can achieve outstanding performance with impressive pre-training efficiency.

5 Conclusion

In this paper, we present a **green** approach for Masked Image Modeling (MIM) with hierarchical Vision Transformers, *e.g.*, Swin Transformer [49] and Twins Transformer [14], allowing the hierarchical models to discard masked patches and operate only on the visible ones. Coupling the efficient Group Window Attention scheme, the DP-algorithm-based Optimal Grouping strategy, and the Sparse Convolution, our approach can train the hierarchical models $\sim 2.7\times$ faster and reduce the GPU memory consumption by up to 70%, while still enjoying a competitive performance on ImageNet classification and the superiority of downstream MS-COCO object detection benchmarks. We hope that this work will facilitate future self-supervised learning methods targeting effectiveness as well as efficiency.

Limitations. One of the limitations of our algorithm is that it requires the batch-wise masking scheme (as in Section 3.5) to achieve the best efficiency. Although this limitation only has little impact on the MIM pre-training, it restrains the application of our method on a broader range of settings, *e.g.*, training ViTs with token sparsification [59, 75] that requires instance-wise sparsification. These applications are beyond the scope of this work and we will leave them for future study.

Broader Impact. This work proposed a green approach for MIM with hierarchical ViTs, prominently alleviating the heavy computation burden of MIM. On the one hand, this work provokes the efficiency as well as the effectiveness of MIM, which may inspire new algorithms and investigations in this direction. On the other hand, since the pre-training datasets might contain biases, our approach, in the same way as other unsupervised/self-supervised learning methods, might also be susceptible to replicating these biases. This concern can be mitigated by combining the FairML methods [4].

References

- [1] spconv. <https://github.com/traveller59/spconv>.
- [2] A. Baevski, W.-N. Hsu, Q. Xu, A. Babu, J. Gu, and M. Auli. Data2vec: A general framework for self-supervised learning in speech, vision and language. *arXiv preprint arXiv:2202.03555*, 2022.
- [3] H. Bao, L. Dong, and F. Wei. Beit: Bert pre-training of image transformers. *arXiv preprint arXiv:2106.08254*, 2021.
- [4] S. Barocas, M. Hardt, and A. Narayanan. Fairness in machine learning. *Nips tutorial*, 1:2, 2017.
- [5] R. Bellman. Dynamic programming. *Science*, 153(3731):34–37, 1966.

- [6] T. B. Brown, B. Mann, N. Ryder, M. Subbiah, J. Kaplan, P. Dhariwal, A. Neelakantan, P. Shyam, G. Sastry, A. Askell, et al. Language models are few-shot learners. In *Advances in Neural Information Processing Systems*, volume 33, 2020.
- [7] M. Caron, I. Misra, J. Mairal, P. Goyal, P. Bojanowski, and A. Joulin. Unsupervised learning of visual features by contrasting cluster assignments. *Advances in Neural Information Processing Systems*, 33, 2020.
- [8] M. Caron, H. Touvron, I. Misra, H. Jégou, J. Mairal, P. Bojanowski, and A. Joulin. Emerging properties in self-supervised vision transformers. *arXiv preprint arXiv:2104.14294*, 2021.
- [9] K. Chen, J. Wang, J. Pang, Y. Cao, Y. Xiong, X. Li, S. Sun, W. Feng, Z. Liu, J. Xu, et al. Mmdetection: Open mmlab detection toolbox and benchmark. *arXiv preprint arXiv:1906.07155*, 2019.
- [10] T. Chen, S. Kornblith, M. Norouzi, and G. Hinton. A simple framework for contrastive learning of visual representations. In *International Conference on Machine Learning*, 2020.
- [11] X. Chen and K. He. Exploring simple Siamese representation learning. *arXiv preprint arXiv:2011.10566*, 2020.
- [12] X. Chen, S. Xie, and K. He. An empirical study of training self-supervised vision transformers. In *Proceedings of the IEEE/CVF International Conference on Computer Vision*, pages 9640–9649, 2021.
- [13] C. Choy, J. Gwak, and S. Savarese. 4d spatio-temporal convnets: Minkowski convolutional neural networks. In *Proceedings of the IEEE/CVF Conference on Computer Vision and Pattern Recognition*, pages 3075–3084, 2019.
- [14] X. Chu, Z. Tian, Y. Wang, B. Zhang, H. Ren, X. Wei, H. Xia, and C. Shen. Twins: Revisiting the design of spatial attention in vision transformers. *Advances in Neural Information Processing Systems*, 34, 2021.
- [15] J. Devlin, M.-W. Chang, K. Lee, and K. Toutanova. Bert: Pre-training of deep bidirectional transformers for language understanding. In *North American Chapter of the Association for Computational Linguistics: Human Language Technologies*, pages 4171–4186, 2019.
- [16] X. Dong, J. Bao, T. Zhang, D. Chen, W. Zhang, L. Yuan, D. Chen, F. Wen, and N. Yu. Peco: Perceptual codebook for bert pre-training of vision transformers. *arXiv preprint arXiv:2111.12710*, 2021.
- [17] A. Dosovitskiy, L. Beyer, A. Kolesnikov, D. Weissenborn, X. Zhai, T. Unterthiner, M. Dehghani, M. Minderoeder, G. Heigold, S. Gelly, et al. An image is worth 16x16 words: Transformers for image recognition at scale. *arXiv preprint arXiv:2010.11929*, 2020.
- [18] S. d’Ascoli, H. Touvron, M. L. Leavitt, A. S. Morcos, G. Biroli, and L. Sagun. Convit: Improving vision transformers with soft convolutional inductive biases. In *International Conference on Machine Learning*, pages 2286–2296. PMLR, 2021.
- [19] H. Fan, B. Xiong, K. Mangalam, Y. Li, Z. Yan, J. Malik, and C. Feichtenhofer. Multiscale vision transformers. In *Proceedings of the IEEE/CVF International Conference on Computer Vision*, pages 6824–6835, 2021.
- [20] G. Ghiasi, Y. Cui, A. Srinivas, R. Qian, T.-Y. Lin, E. D. Cubuk, Q. V. Le, and B. Zoph. Simple copy-paste is a strong data augmentation method for instance segmentation. In *Proceedings of the IEEE/CVF Conference on Computer Vision and Pattern Recognition*, pages 2918–2928, 2021.
- [21] S. Gidaris, P. Singh, and N. Komodakis. Unsupervised representation learning by predicting image rotations. In *International Conference on Learning Representation*, 2018.
- [22] R. Girshick, J. Donahue, T. Darrell, and J. Malik. Rich feature hierarchies for accurate object detection and semantic segmentation. In *IEEE Conference on Computer Vision and Pattern Recognition*, pages 580–587, 2014.
- [23] I. Goodfellow, J. Pouget-Abadie, M. Mirza, B. Xu, D. Warde-Farley, S. Ozair, A. Courville, and Y. Bengio. Generative adversarial nets. In *Advances in Neural Information Processing Systems*, pages 2672–2680, 2014.
- [24] B. Graham. Sparse 3d convolutional neural networks. *arXiv preprint arXiv:1505.02890*, 2015.
- [25] B. Graham, M. Engelcke, and L. Van Der Maaten. 3d semantic segmentation with submanifold sparse convolutional networks. In *Proceedings of the IEEE conference on computer vision and pattern recognition*, pages 9224–9232, 2018.
- [26] J.-B. Grill, F. Strub, F. Altché, C. Tallec, P. Richemond, E. Buchatskaya, C. Doersch, B. Avila Pires, Z. Guo, M. Gheshlaghi Azar, et al. Bootstrap your own latent: A new approach to self-supervised learning. *Advances in Neural Information Processing Systems*, 33, 2020.
- [27] J. Guo, K. Han, H. Wu, Y. Tang, X. Chen, Y. Wang, and C. Xu. Cmt: Convolutional neural networks meet vision transformers. In *Proceedings of the IEEE/CVF Conference on Computer Vision and Pattern Recognition*, pages 12175–12185, 2022.
- [28] K. He, X. Chen, S. Xie, Y. Li, P. Dollár, and R. Girshick. Masked autoencoders are scalable vision learners. *arXiv preprint arXiv:2111.06377*, 2021.

- [29] K. He, H. Fan, Y. Wu, S. Xie, and R. Girshick. Momentum contrast for unsupervised visual representation learning. In *IEEE Conference on Computer Vision and Pattern Recognition*, pages 9729–9738, 2020.
- [30] K. He, G. Gkioxari, P. Dollár, and R. Girshick. Mask r-cnn. In *Proceedings of the IEEE international conference on computer vision*, pages 2961–2969, 2017.
- [31] K. He, X. Zhang, S. Ren, and J. Sun. Deep residual learning for image recognition. In *IEEE Conference on Computer Vision and Pattern Recognition*, pages 770–778, 2016.
- [32] O. J. Hénaff, S. Koppula, J.-B. Alayrac, A. v. d. Oord, O. Vinyals, and J. Carreira. Efficient visual pretraining with contrastive detection. *arXiv preprint arXiv:2103.10957*, 2021.
- [33] J. Ho, A. Jain, and P. Abbeel. Denoising diffusion probabilistic models. *Advances in Neural Information Processing Systems*, 33:6840–6851, 2020.
- [34] G. Huang, Y. Sun, Z. Liu, D. Sedra, and K. Q. Weinberger. Deep networks with stochastic depth. In *European Conference on Computer Vision*, pages 646–661. Springer, 2016.
- [35] L. Huang, S. You, M. Zheng, F. Wang, C. Qian, and T. Yamasaki. Learning where to learn in cross-view self-supervised learning. In *Proceedings of the IEEE/CVF Conference on Computer Vision and Pattern Recognition*, pages 14451–14460, 2022.
- [36] L. Huang, Y. Yuan, J. Guo, C. Zhang, X. Chen, and J. Wang. Interlaced sparse self-attention for semantic segmentation. *arXiv preprint arXiv:1907.12273*, 2019.
- [37] L. Huang, C. Zhang, and H. Zhang. Self-adaptive training: Bridging supervised and self-supervised learning. *arXiv preprint arXiv:2101.08732*, 2021.
- [38] Z. Huang, Y. Ben, G. Luo, P. Cheng, G. Yu, and B. Fu. Shuffle transformer: Rethinking spatial shuffle for vision transformer. *arXiv preprint arXiv:2106.03650*, 2021.
- [39] T. Karras, S. Laine, and T. Aila. A style-based generator architecture for generative adversarial networks. In *Proceedings of the IEEE/CVF conference on computer vision and pattern recognition*, pages 4401–4410, 2019.
- [40] H. Kellerer, U. Pferschy, and D. Pisinger. *Knapsack problems*. Springer, 2004.
- [41] D. P. Kingma and J. Ba. Adam: A method for stochastic optimization. In *International Conference on Learning Representations*, 2015.
- [42] D. P. Kingma and M. Welling. Auto-encoding variational Bayes. In *International Conference on Learning Representations*, 2014.
- [43] A. Krizhevsky, I. Sutskever, and G. E. Hinton. Imagenet classification with deep convolutional neural networks. In *Advances in Neural Information Processing Systems*, volume 25, pages 1097–1105, 2012.
- [44] G. Larsson, M. Maire, and G. Shakhnarovich. Colorization as a proxy task for visual understanding. In *Proceedings of the IEEE conference on computer vision and pattern recognition*, pages 6874–6883, 2017.
- [45] Y. Li, S. Xie, X. Chen, P. Dollar, K. He, and R. Girshick. Benchmarking detection transfer learning with vision transformers. *arXiv preprint arXiv:2111.11429*, 2021.
- [46] T.-Y. Lin, P. Dollár, R. Girshick, K. He, B. Hariharan, and S. Belongie. Feature pyramid networks for object detection. In *Proceedings of the IEEE conference on computer vision and pattern recognition*, pages 2117–2125, 2017.
- [47] T.-Y. Lin, M. Maire, S. Belongie, J. Hays, P. Perona, D. Ramanan, P. Dollár, and C. L. Zitnick. Microsoft coco: Common objects in context. In *European conference on computer vision*, pages 740–755. Springer, 2014.
- [48] Z. Liu, H. Hu, Y. Lin, Z. Yao, Z. Xie, Y. Wei, J. Ning, Y. Cao, Z. Zhang, L. Dong, et al. Swin transformer v2: Scaling up capacity and resolution. *arXiv preprint arXiv:2111.09883*, 2021.
- [49] Z. Liu, Y. Lin, Y. Cao, H. Hu, Y. Wei, Z. Zhang, S. Lin, and B. Guo. Swin transformer: Hierarchical vision transformer using shifted windows. In *Proceedings of the IEEE/CVF International Conference on Computer Vision*, pages 10012–10022, 2021.
- [50] I. Loshchilov and F. Hutter. SGDR: Stochastic gradient descent with warm restarts. In *International Conference on Learning Representations*, 2017.
- [51] P. Micikevicius, S. Narang, J. Alben, G. Diamos, E. Elsen, D. Garcia, B. Ginsburg, M. Houston, O. Kuchaiev, G. Venkatesh, et al. Mixed precision training. *arXiv preprint arXiv:1710.03740*, 2017.
- [52] M. Noroozi and P. Favaro. Unsupervised learning of visual representations by solving jigsaw puzzles. In *European Conference on Computer Vision*, pages 69–84. Springer, 2016.
- [53] A. v. d. Oord, Y. Li, and O. Vinyals. Representation learning with contrastive predictive coding. *arXiv preprint arXiv:1807.03748*, 2018.

- [54] A. Paszke, S. Gross, F. Massa, A. Lerer, J. Bradbury, G. Chanan, T. Killeen, Z. Lin, N. Gimelshein, L. Antiga, et al. Pytorch: An imperative style, high-performance deep learning library. In *Advances in Neural Information Processing Systems*, pages 8024–8035, 2019.
- [55] D. Pathak, P. Krahenbuhl, J. Donahue, T. Darrell, and A. A. Efros. Context encoders: Feature learning by inpainting. In *IEEE Conference on Computer Vision and Pattern Recognition*, pages 2536–2544, 2016.
- [56] A. Radford, K. Narasimhan, T. Salimans, and I. Sutskever. Improving language understanding by generative pre-training, 2018.
- [57] A. Radford, J. Wu, R. Child, D. Luan, D. Amodei, and I. Sutskever. Language models are unsupervised multitask learners. *OpenAI blog*, 1(8):9, 2019.
- [58] A. Ramesh, M. Pavlov, G. Goh, S. Gray, C. Voss, A. Radford, M. Chen, and I. Sutskever. Zero-shot text-to-image generation. In *International Conference on Machine Learning*, pages 8821–8831. PMLR, 2021.
- [59] Y. Rao, W. Zhao, B. Liu, J. Lu, J. Zhou, and C.-J. Hsieh. Dynamicvit: Efficient vision transformers with dynamic token sparsification. *Advances in neural information processing systems*, 34, 2021.
- [60] O. Russakovsky, J. Deng, H. Su, J. Krause, S. Satheesh, S. Ma, Z. Huang, A. Karpathy, A. Khosla, M. Bernstein, et al. Imagenet large scale visual recognition challenge. *International Journal of Computer Vision*, 115(3):211–252, 2015.
- [61] R. Schwartz, J. Dodge, N. A. Smith, and O. Etzioni. Green ai. *Communications of the ACM*, 63(12):54–63, 2020.
- [62] H. Touvron, M. Cord, M. Douze, F. Massa, A. Sablayrolles, and H. Jégou. Training data-efficient image transformers & distillation through attention. In *International Conference on Machine Learning*, pages 10347–10357. PMLR, 2021.
- [63] A. Van Den Oord, O. Vinyals, et al. Neural discrete representation learning. *Advances in neural information processing systems*, 30, 2017.
- [64] A. Vaswani, N. Shazeer, N. Parmar, J. Uszkoreit, L. Jones, A. N. Gomez, Ł. Kaiser, and I. Polosukhin. Attention is all you need. *Advances in neural information processing systems*, 30, 2017.
- [65] P. Vincent, H. Larochelle, Y. Bengio, and P.-A. Manzagol. Extracting and composing robust features with denoising autoencoders. In *International Conference on Machine Learning*, pages 1096–1103, 2008.
- [66] W. Wang, E. Xie, X. Li, D.-P. Fan, K. Song, D. Liang, T. Lu, P. Luo, and L. Shao. Pyramid vision transformer: A versatile backbone for dense prediction without convolutions. In *Proceedings of the IEEE/CVF International Conference on Computer Vision*, pages 568–578, 2021.
- [67] X. Wang, R. Zhang, C. Shen, T. Kong, and L. Li. Dense contrastive learning for self-supervised visual pre-training. In *Proceedings of the IEEE/CVF Conference on Computer Vision and Pattern Recognition*, pages 3024–3033, 2021.
- [68] C. Wei, H. Fan, S. Xie, C.-Y. Wu, A. Yuille, and C. Feichtenhofer. Masked feature prediction for self-supervised visual pre-training. *arXiv preprint arXiv:2112.09133*, 2021.
- [69] H. Wu, B. Xiao, N. Codella, M. Liu, X. Dai, L. Yuan, and L. Zhang. Cvt: Introducing convolutions to vision transformers. In *Proceedings of the IEEE/CVF International Conference on Computer Vision*, pages 22–31, 2021.
- [70] Z. Wu, Y. Xiong, S. X. Yu, and D. Lin. Unsupervised feature learning via non-parametric instance discrimination. In *IEEE Conference on Computer Vision and Pattern Recognition*, pages 3733–3742, 2018.
- [71] T. Xiao, C. J. Reed, X. Wang, K. Keutzer, and T. Darrell. Region similarity representation learning. *arXiv preprint arXiv:2103.12902*, 2021.
- [72] Z. Xie, Y. Lin, Z. Zhang, Y. Cao, S. Lin, and H. Hu. Propagate yourself: Exploring pixel-level consistency for unsupervised visual representation learning. In *Proceedings of the IEEE/CVF Conference on Computer Vision and Pattern Recognition*, pages 16684–16693, 2021.
- [73] Z. Xie, Z. Zhang, Y. Cao, Y. Lin, J. Bao, Z. Yao, Q. Dai, and H. Hu. Simmim: A simple framework for masked image modeling. *arXiv preprint arXiv:2111.09886*, 2021.
- [74] J. Xu, W. Zhou, Z. Fu, H. Zhou, and L. Li. A survey on green deep learning. *arXiv preprint arXiv:2111.05193*, 2021.
- [75] H. Yin, A. Vahdat, J. Alvarez, A. Mallya, J. Kautz, and P. Molchanov. Adavit: Adaptive tokens for efficient vision transformer. *arXiv preprint arXiv:2112.07658*, 2021.
- [76] W. Yu, M. Luo, P. Zhou, C. Si, Y. Zhou, X. Wang, J. Feng, and S. Yan. Metaformer is actually what you need for vision. In *Proceedings of the IEEE/CVF Conference on Computer Vision and Pattern Recognition*, pages 10819–10829, 2022.

- [77] Y. Yuan, R. Fu, L. Huang, W. Lin, C. Zhang, X. Chen, and J. Wang. Hrformer: High-resolution vision transformer for dense predict. *Advances in Neural Information Processing Systems*, 34, 2021.
- [78] J. Zbontar, L. Jing, I. Misra, Y. LeCun, and S. Deny. Barlow twins: Self-supervised learning via redundancy reduction. *arXiv preprint arXiv:2103.03230*, 2021.
- [79] M. Zheng, F. Wang, S. You, C. Qian, C. Zhang, X. Wang, and C. Xu. Weakly supervised contrastive learning. In *Proceedings of the IEEE/CVF International Conference on Computer Vision (ICCV)*, pages 10042–10051, October 2021.
- [80] M. Zheng, S. You, F. Wang, C. Qian, C. Zhang, X. Wang, and C. Xu. Rssl: Relational self-supervised learning with weak augmentation. *Advances in Neural Information Processing Systems*, 34, 2021.
- [81] J. Zhou, C. Wei, H. Wang, W. Shen, C. Xie, A. Yuille, and T. Kong. ibot: Image bert pre-training with online tokenizer. *arXiv preprint arXiv:2111.07832*, 2021.

Checklist

1. For all authors...
 - (a) Do the main claims made in the abstract and introduction accurately reflect the paper’s contributions and scope? [\[Yes\]](#)
 - (b) Did you describe the limitations of your work? [\[Yes\]](#) In the supplemental materials.
 - (c) Did you discuss any potential negative societal impacts of your work? [\[Yes\]](#) In the supplemental materials.
 - (d) Have you read the ethics review guidelines and ensured that your paper conforms to them? [\[Yes\]](#)
2. If you are including theoretical results...
 - (a) Did you state the full set of assumptions of all theoretical results? [\[N/A\]](#)
 - (b) Did you include complete proofs of all theoretical results? [\[N/A\]](#)
3. If you ran experiments...
 - (a) Did you include the code, data, and instructions needed to reproduce the main experimental results (either in the supplemental material or as a URL)? [\[Yes\]](#)
 - (b) Did you specify all the training details (e.g., data splits, hyperparameters, how they were chosen)? [\[Yes\]](#)
 - (c) Did you report error bars (e.g., with respect to the random seed after running experiments multiple times)? [\[No\]](#)
 - (d) Did you include the total amount of compute and the type of resources used (e.g., type of GPUs, internal cluster, or cloud provider)? [\[Yes\]](#)
4. If you are using existing assets (e.g., code, data, models) or curating/releasing new assets...
 - (a) If your work uses existing assets, did you cite the creators? [\[Yes\]](#)
 - (b) Did you mention the license of the assets? [\[Yes\]](#)
 - (c) Did you include any new assets either in the supplemental material or as a URL? [\[No\]](#)
 - (d) Did you discuss whether and how consent was obtained from people whose data you’re using/curating? [\[N/A\]](#)
 - (e) Did you discuss whether the data you are using/curating contains personally identifiable information or offensive content? [\[N/A\]](#)
5. If you used crowdsourcing or conducted research with human subjects...
 - (a) Did you include the full text of instructions given to participants and screenshots, if applicable? [\[N/A\]](#)
 - (b) Did you describe any potential participant risks, with links to Institutional Review Board (IRB) approvals, if applicable? [\[N/A\]](#)
 - (c) Did you include the estimated hourly wage paid to participants and the total amount spent on participant compensation? [\[N/A\]](#)

Table 4: Influence of the optimal grouping on Group Window Attention.

Group size g_s	Dynamic Programming	FLOPS@Stage1	FLOPS@Stage1	FLOPS@Stage1
Greedy (Algorithm 1)	✓	62.6M	55.4M	52.3M
$p \times p$ (i.e., 49)	✓	65.0M	58.5M	52.7M
$\max_i w_i$	✓	64.5M	59.7M	62.5M
$\max_i w_i$	×	137.5M	113.3M	75.7M
$\sum_i w_i$	×	201.3M	69.2M	52.7M

Table 5: Time cost of each component in the Group Window Attention.

Time Cost (ms)	DP	Masking	Pre-proc	Grouping	Ungrouping	Attention Fwd & Bwd
Stage1	4.9	3.8	14.8	0.4	0.4	61.9
Stage2	0.6	0.1	2.1	0.2	0.2	20.8
Stage3	0.1	0.1	1.0	0.1	0.1	15.4

A More Ablation Studies

A.1 Efficiency comparison using Twins-L

Here we compare our method with a variant of MAE that operates on both visible and masked patches, which is almost identical to SimMIM except for the choice of the loss function. As shown in Table 6, our method performs on par with the baseline MAE operating on all patches while enjoying 2.6x pre-training speedup in a greener way.

Table 6: Comparison using Twins-L.

Method	Time	Mem.	Acc.
MAE w/ all patches	2.6h	408.3G	83.5%
Ours	0.8h	102.3G	83.3%

A.2 Analysis on the Optimal Grouping

Following the setting in Figure 4, we compare the complexity of a single group attention module, w/ or w/o dynamic programming, at each stage as below. As displayed in Table 4, when $g_s = \max_i w_i$, the complexity is doubled without the DP solver. Simply setting $g_s = \sum_i w_i$ (such that there is only 1 group) also suffers from heavy cost, encountering an out-of-memory error in practice even with a much smaller batch size (e.g., 64 per GPU). In contrast, with the DP solver, the complexity is significantly reduced even when we simply fix the group size to the same as the window size $p \times p$ (note that $\max_i w_i = p \times p$ with a high probability in practice) as discussed in Sec. 4.2. This experiment demonstrates the efficacy of our optimal grouping scheme.

In addition, We benchmark the time cost (ms) of each component in a single Group Attention module and summarize the results in Table 5. Here we use a tensor of shape $[256, H_i \times W_i, C_i]$ as input, where H_i, W_i, C_i denote the height, width, and the number of channels of the features in the i th stage. Note that the DP, masking, and other pre-processing operations are only executed twice for each stage, i.e., for the shifted/unshifted window partition. We can see that the extra cost of our method is indeed moderate compared with the attention computation.

B More Details of Our Method

B.1 Method Overview.

We provide a diagram in Figure 6 for an intuitive illustration of our method. The input image is first randomly masked according to the masking scheme in Section 3.5, then fed into our green hierarchical ViT to obtain representations for each visible patch. Finally, we concatenate the representations of visible patches with the mask tokens and feed them into a transformer decoder, yielding the representations for the masked patches. Finally, we predict the raw pixel values of masked patches

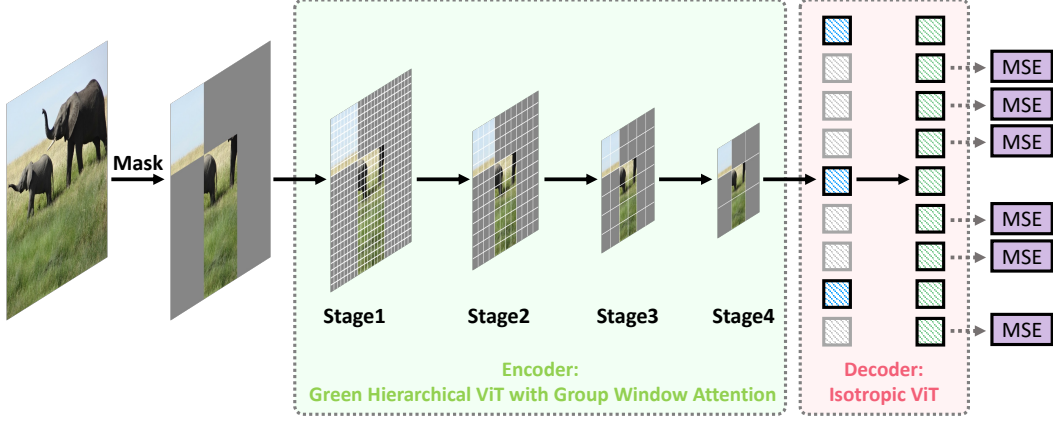


Figure 6: **Overview of our method.** The input image is randomly masked and then fed into a 4-stage hierarchical ViTs. Finally, a lightweight decoder takes the representations of visible patches and mask tokens to reconstruct the missing patches.

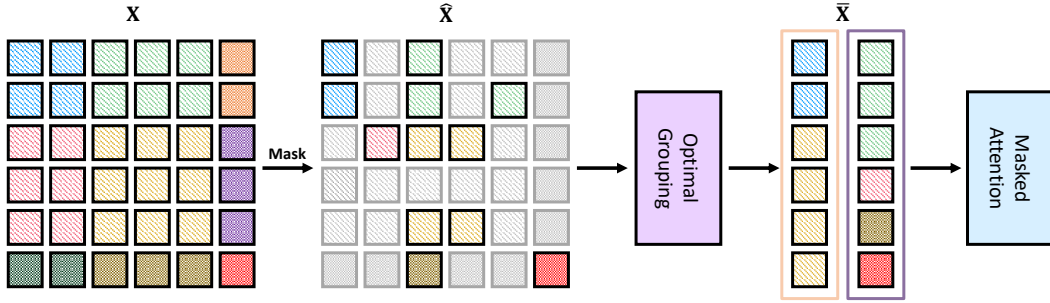


Figure 7: **Illustration of the Group Window Attention scheme with shifted windows.** It shows that our approach is agnostic to the window partition.

from the corresponding representations and implement the training by minimizing the Mean Square Error (MSE) between the predictions and ground truth.

B.2 Group Window Attention scheme with shifted windows.

In addition to Figure 2, we also illustrate how our method works with the irregular window partition in Figure 7. We can observe that owing to the optimal grouping scheme, our method dynamically finds out the best group partition despite the number of visible patches within each local window being highly uneven. This figure further demonstrates that our approach is agnostic to the window partition and works impressively well.

B.3 A Python Implementation of the Optimal Grouping algorithm

We provide a Python implementation of the Dynamic-Programming-based Optimal Grouping algorithm in Algorithm 2. As we can see, the two components of the Optimal Grouping algorithm are both easy to implement. For the DP algorithm for the single Knapsack problem, its time/space complexity is $\mathcal{O}(g_s n_w)$ where g_s is the group size and n_w is the number of windows. In practice, because g_s and n_w are generally small (*i.e.*, smaller than 100) the running time of Algorithm 2 is negligible (*i.e.*, $< 1\text{ms}$).

B.4 A PyTorch Implementation of the Group Attention scheme

With the group partition on the indexes, we can then permute visible patches according to the partition and obtain several groups of patches with an equal size g_s , upon which the Masked Attention is

Algorithm 2 Dynamic Programming-based algorithm for the Optimal Grouping using Python.

```
1 def Knapsack(g_s, Phi):
2     # g_s (int): Group size
3     # Phi (list[int]): The numbers of visible patches within each local window
4
5     n_w = len(Phi) # the number of windows
6     K = [[0 for w in range(g_s + 1)] for i in range(n_w + 1)] # a buffer for the DP
       algorithm
7
8     # Build table K[][] in a bottom up manner
9     for i in range(n_w + 1):
10         for w in range(g_s + 1):
11             if i == 0 or w == 0:
12                 K[i][w] = 0
13             elif Phi[i - 1] <= w:
14                 K[i][w] = max(Phi[i - 1] + K[i - 1][w - Phi[i - 1]], K[i - 1][w])
15             else:
16                 K[i][w] = K[i - 1][w]
17
18     # Store the result of Knapsack
19     res = K[n_w][g_s]
20
21     # Store the selected indexes
22     w = g_s
23     Pi = []
24
25     for i in range(n_w, 0, -1):
26         if res <= 0:
27             break
28
29         if res == K[i - 1][w]: # This window is not included.
30             continue
31         else: # This window is included.
32             Pi.append(i - 1)
33             # Since this window is included, its value is deducted
34             res = res - Phi[i - 1]
35             w = w - Phi[i - 1]
36
37     return Pi[::-1] # Optional: make Pi in an increasing order
38
39
40 def GroupPartition(g_s, Phi):
41     # g_s (int): Group size
42     # Phi (list[int]): The numbers of visible patches within each local window
43
44     win_szs = Phi.copy()
45     ori_win_idx = list(range(len(win_szs)))
46     win_idx = []
47
48     while len(win_szs) > 0:
49         idx = knapsack(group_size, win_szs)
50
51         # Append the selected idx
52         win_idx.append([ori_win_idx[i] for i in idx])
53
54         # The remaining windows and indexes
55         win_szs = [win_szs[i] for i in range(len(ori_win_idx)) if i not in idx]
56         ori_win_idx = [ori_win_idx[i] for i in range(len(ori_win_idx)) if i not in idx]
57
58     return win_idx
```

performed. We also provide a PyTorch implementation of the Group Attention scheme in Algorithm 3 to facilitate future research. Note the padding operations are omitted here for simplicity.

Algorithm 3 Group Attention using the PyTorch framework.

```
1 def GroupAttention(x, g_s, Phi):
2     # x (3-d tensor): Features the visible patches
3     # g_s (int): Group size
4     # Phi (list[int]): The numbers of visible patches within each local window
5
6     # B is the batch size, L is the number of visible patches, C is the number of channels
7     B, L, C = x.shape
8
9     # Prepare for the group attention
10    win_idx = GroupPartition(g_s, Phi)
11    patch_idx = torch.arange(sum(Phi))
12    patch_idx = torch.split(patch_idx, Phi)
13    shuffle_idx = torch.cat([patch_idx[wi] for wi in win_idx])
14    unshuffle_idx = torch.argsort(shuffle_idx)
15
16    # Group partition. For simplicity, assume that the partition is even
17    x = torch.index_select(x, 1, shuffle_idx) # (B, n_g * g_s, C)
18    x = x.reshape(-1, g_s, C) # (B * n_g, g_s, C)
19
20    # Attention with relative position bias as in Figure 3
21    x = MaskedAttention(x)
22
23    # Reverse the group partition
24    x = x.reshape(B, L, C).index_select(x, 1, unshuffle_idx)
25
26    return x
```
